JOURNAL OF PHYSICAL ORGANIC CHEMISTRY
*J. Phys. Org. Chem.* **12,** 10–18 (1999)

# Semiempirical computational assessment of porphyrins as building blocks for molecule-based magnets: spin–spin coupling in radical-substituted metalloporphyrins

**David A. Shultz, Kay A. Sandberg**

[1]Department of Chemistry, North Carolina State University, Raleigh, North Carolina 27695-8204, USA

*Received 23 January 1998; revised 16 March 1998; accepted 24 March 1998*

ABSTRACT: Semiempirical PM3-RHF-CI calculations were used to probe structure–exchange coupling relationships in radical-substituted Zn(II) porphyrins. The results support a number of important design elements for creating high-spin molecules from metalloporphyrins and the corresponding pi-cation radicals. The calculations showed that inactive porphyrin–active phenoxy union mode provides stronger exchange coupling than active porphyrin–inactive phenoxy union mode. Connecting radicals to the metalloporphyrin core via an ethynyl linkage eliminates severe torsion, permitting a coplanar alignment of the two pi systems. Metalloporphyrins could be excellent redox-activated exchange couplers: porphyrin radical cation exchange couples attached radicals more effectively than the neutral porphyrin. Finally, the magnitude of exchange coupling between a metalloporphyrin pi-cation radical depends on the nature of the attached radical. The results of the calculations were explained using a coupler spin analysis. Copyright © 1999 John Wiley & Sons, Ltd.

KEYWORDS: Porphyrins; radical-substituted metalloporphyrins; molecule-based magnets; spin–spin coupling

Developing molecule-based systems capable of exhibiting magnetic ordering with the ultimate goal of bulk magnetic behavior is an active area of research.[1] A molecular magnet is defined as a bulk magnetic system in which at least one of its magnetic components arises from spin sites in either s- or p- orbitals.[2] One strategy for designing a potential molecular magnetic system is to design high-spin building blocks—molecules containing ferromagnetically coupled unpaired spins—that are subsequently magnetically coupled as illustrated below.[3] The magnetic coupling mechanism can operate through hydrogen bonds, conjugated pi systems, metal ligation or through-space interactions.[4–11]

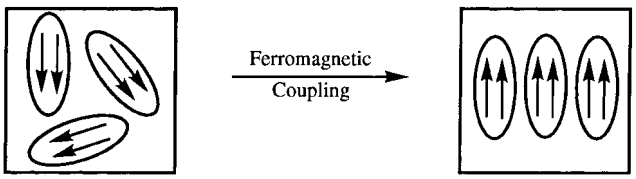


An accepted strategy for molecular and supramolecular design is coupling of spin-containing units (SCU) with a ferromagnetic coupling unit (FCU).[12] The SCU is any stable species with a permanent magnetic moment. The FCU is any linker that promotes the parallel alignment of the magnetic moments (*i.e.* stabilizes the high-spin state). Here, we investigated the effectiveness of the metalloporphyrin and its radical cation as FCUs using a computational approach.


Multispin molecular assemblies featuring metalloporphyrins are promising components of molecule-based magnetic materials. Interesting molecules and building blocks include porphyrins with phenylcarbene groups whose spin–spin coupling depends on the substitution pattern.[13,14] Kamachi[15] reported verdazyl-substituted porphyrins attached to polymer backbones that exhibit weak antiferromagnetic interactions.[13] Kitano *et al.*[16] studied the magnetic behavior of pyridine nitroxides coordinated to chromium(III) tetraphenylporphyrin. Miller *et al.*[17] are studying a series of Mn(II) porphyrin–TCNE complexes that order magnetically at surprising high temperatures.[18]

We are preparing radical-substituted metalloporphyrins for the construction of coordination polymers with interesting magnetic properties[19,20] (hereafter, 'porphyrin' refers to metalloporphyrin). Porphyrins are attractive from a synthetic point of view for four reasons: (1) there are 12 positions at which substituents can be attached, *i.e.*

**Correspondence to:* D. A. Shultz, Department of Chemistry, North Carolina State University, Raleigh, North Carolina 27695-8204, USA.
*Contract/grant sponsor:* National Science Foundation; *Contract/grant number:* CHE-9501085.


CCC 0894–3230/99/010010–09 $17.50

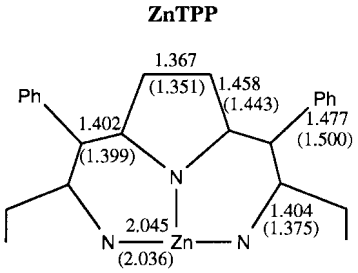


**Figure 1.** Calculated and experimental[38] bond lengths for ZnTPP

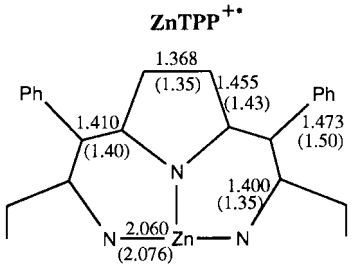


**Figure 2.** Calculated and experimental[44] bond lengths for $ZnTPP^{+\cdot}$

four *meso*-positions and eight $\beta$-pyrrole positions, (2) the coordination of metals in the center of the macrocycle provides a handle for synthesizing extended systems, (3) the redox properties are well understood and (4) the electronic character of the oxidized porphyrin is conducive to spin–spin coupling. There are several design motifs for spin–spin coupling in such molecules, including coupling an attached organic radical spin with the unpaired electron of an oxidized porphyrin, coupling with a transition metal spin or coupling with both.

We desire a theoretical foundation and need to test topological models for spin–spin coupling in these novel structures. Because the systems under investigation are large and contain several heteroatoms, high-level *ab initio* calculations are not practical and therefore we have necessarily relied upon semiempirical calculations to make predictions and draw conclusions. Semiempirical methods have proven useful for understanding trends in organic polyradicals[21–27] and probing the structures and electronic properties of porphyrins.[28–32]

The paper is divided into four parts. The first part focuses on the ferromagnetic coupling of a single organic radical spin with the unpaired electron of the porphyrin radical cation propagated through the *meta*-through-a-benzene union mode leading to $S = 1$ species. The second part demonstrates the ferromagnetic coupling of peripheral organic radical spins by the ferromagnetic coupling of each to the unpaired electron of the porphyrin radical cation resulting in $S = 3/2$ species. Since the coupling is propagated through a redox-active species, we refer to it as 'redox-activated exchange coupling.' In this case the FCU ($ZnTPP^{+\cdot}$) is also an SCU. The third part shows the lack of significant coupling when the neutral metalloporphyrin, ZnTPP, is used as the FCU. Finally, we compare the coupling of $ZnTPP^{+\cdot}$ with two common, stable SCUs: galvinoxyl and nitronylnitroxide.

A successful, systematic approach to investigating the spin–spin coupling strength of an FCU is to (1) choose an SCU to be used throughout the study and (2) vary the FCU by either modifying its molecular structure or altering the SCU–FCU connectivity.[33] As mentioned above, the unique FCUs under investigation are the metalloporphyrin (ZnTPP) and the corresponding metalloporphyrin radical cation ($ZnTPP^{+\cdot}$). We chose the oxy radical as the SCU. Lahti and co-workers[23,25,26] have used the oxy radical as the SCU in computational investigations of the effectiveness of other magnetic couplers and found the results to be in qualitative agreement with experiment. Here, we describe the results of PM3-RHF-CI[34] calculations on radical-substituted $ZnTPP^{+\cdot}$ and radical-substituted ZnTPP.

Like other computational investigations, certain constraints and assumptions are made for the sake of computational efficiency which preclude obtaining definitive quantitative results, but allow qualitative and semiquantitative conclusions to be reached.[21,22,26,27,29,30,35–37] Zinc(II) tetraphenylporphyrin (ZnTPP) and zinc(II) tetraphenylporphyrin radical cation ($ZnTPP^{+\cdot}$) geometries were obtained from UHF-PM3 optimizations subject to both symmetry and planar constraints.[38,39] As noted previously, UHF calculations on high-spin molecules are more likely to provide accurate geometries than RHF calculations.[40] The crystallographic coordinates of $[Mg(TPP)aquo]^{+\cdot}$ were used as the initial geometry[41] replacing Mg with Zn and placing the Zn atom in the center of the macrocycle.[42] As shown in Figs 1 and 2 optimized bond lengths, angles and dihedrals are consistent with those reported in the literature for ZnTPP and $ZnTPP^{+\cdot}$, respectively.[43,44] The optimized Zn—$N_{pyrrole}$ bond distance is 2.06 Å for $ZnTPP^{+\cdot}$ and 2.05 Å for ZnTPP compared with the crystallographic lengths of 2.06–2.09 Å for $ZnTPP^{+\cdot}$[45] and 2.05 Å for ZnTPP.[44] The optimized $C_{meso}$—$C(1')_{(phenyl)}$ bond length and phenyl-core dihedral angle for $ZnTPP^{+\cdot}$ are 1.47 Å and 67°, respectively, compared with 1.48–1.51 Å and 49.8–68.4° obtained from crystallographic studies of $ZnTPPClO_4$[45], and for ZnTPP 1.48 Å and 90° compared with 1.50 Å and 60° obtained from crystallographic studies of ZnTPP.[46]

We found a mere 0.32 kcal $mol^{-1}$ (1 kcal = 4.184 kJ) difference between the energy of the optimized ZnTPP where the phenyl ring-core dihedral angle was 90° and the energy of the optimized structure where the phenyl ring-core dihedral angle was constrained to 67°, illustrating the low energy barrier to rotation. For the sake of consistency we fixed all *meso*-phenyl torsions in this study at 67° in keeping with the geometry of the radical cation.

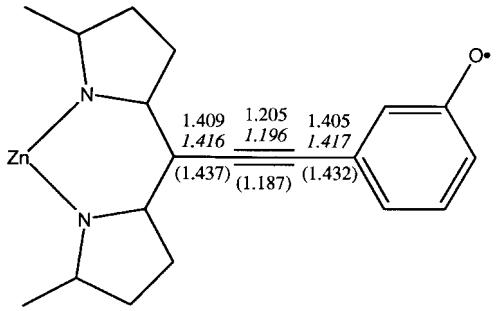


**Figure 3.** Calculated and experimental bond lengths for ethynyl-bridged biradicals. Values in roman type are the calculated lengths for the unoxidized porphyrin those in italics are calculated lengths for the oxidized porphyrin and those in parentheses are from crystallographic data[36]

The SCUs and bridges attached to the porphyrin were optimized subject to planar constraints and symmetry constraints (where appropriate) using the UHF-PM3 Hamiltonian[34] at the highest multiplicity and a planar porphyrin core geometry. As noted previously by Lahti *et al.*,[26] semiempirical calculations are insufficient for making definitive quantitative predictions, but are effective as a tool to predict qualitative trends. They found the separate optimization of the spin states did not produce large differences in the relative energy separations of these states[25] (see Ref. 22 for a discussion of singlet/triplet orbital descriptions). As shown in Fig. 3, for zinc(II) [5-[(3′-oxyphenyl)ethynyl]-10,15,20-triphenylporphyrin] and its radical cation, the optimized $C(5)_{meso}$—$C_{\alpha(\text{ethynyl})}$, $C_{\alpha(\text{ethynyl})}$—$C_{\beta(\text{ethynyl})}$, and $C_{\beta(\text{ethynyl})}$ to $C(1')_{(\text{phenyl})}$ bond lengths (1.409, 1.205, 1.405 Å for unoxidized; 1.416, 1.196, 1.417 Å for oxidized, respectively) are similar to those obtained from the crystallographic data of zinc(II) [5,15-[bis[(4′-methoxyphenyl) ethynyl]-10,20-diphenylporphyrin] (1.437, 1.187, 1.432 Å, respectively).[36] Likewise, the optimized phenoxyethynylporphyrin core dihedral is nearly 0° consistent with the crystallographic data for zinc(II) bis[(4′-methoxyphenyl)ethynyl]-10,20-diphenylporphyrin.

We used spin densities obtained from PM3-RHF-CI[34] calculations in this study since UHF-calculated spin densities are often contaminated.[21] PM3-RHF-CI calculated spin densities for $ZnTPP^{+\cdot}$ are consistent with other calculated values cited in the literature. The calculated *meso*-C and α-C spin densities in this study are 0.125 and 0.0060, respectively, compared with the previously calculated spin densities of 0.193 (0.158) and −0.0094 (0.0066) with CI (without CI).[47] Spin densities for our SCUs are shown in Fig. 4. The calculated spin densities of the *meta*-and *para*-positions of the phenoxy ring are −0.0529 and 0.2969, respectively, which are consistent with the experimental values of −0.0676 and 0.3239.[48] The calculated spin density of the phenoxy ring shows an alternating distribution of spin density consistent with other calculated results.[25,26] The calculated spin densities of the ethynyl-linked nitronylnitroxide atoms are 0.29 (N), 0.20 (O) and 0.0093 ($C_{\text{methine}}$) compared with the experimental values of 0.27 (N), 0.27 (O) and −0.11 ($C_{\text{methine}}$) which were obtained from phenylnitronylnitroxide.[49] The calculated spin densities of the ethynyl-linked galvinoxyl atoms are −0.0061 ($C_{\text{methine}}$), 0.2336 ($C_{ipso}$), −0.0014 ($C_{ortho}$), 0.1204 ($C_{meta}$), 0.0090 ($C_{para}$) and 0.0755 (O) compared with the McLachlan MO calculated spin densities of −0.062 ($C_{\text{methine}}$), 0.153 ($C_{ipso}$), −0.043 ($C_{ortho}$), 0.142 ($C_{meta}$), 0.027 ($C_{para}$) and 0.168 (O) for the phenylgalvinoxy radical.[50,51]

The low-spin–high-spin energy difference, $\Delta E_{\text{LS–HS}}$, was obtained from a PM3-RHF-CI calculation using the keyword OPEN($n$,$n$) where $n = 2$ and 3 for triplet and quartet, respectively. A CI active space of five orbitals was used: two doubly occupied, two singly occupied and one unoccupied for triplets and one doubly occupied, three singly occupied and one unoccupied for quartets. This method has been used previously by other research groups to obtain results that are in qualitative agreement with experiment.[21,27]

Coupling of an attached organic radical with the porphyrin radical cation provides a means of creating $S > 1/2$ species. This feature is a major component of our investigation. As illustrated in Fig. 5, the SOMO of a metalloporphyrin radical cation can have either predominantly $a_{1u}$ or $a_{2u}$ character, depending on which of these two orbitals is higher in energy. In general, oxidation of a *meso*-substituted metalloporphyrin results in the removal of an electron from the $a_{2u}$ orbital leaving unpaired spin density concentrated at the *meso* carbons and pyrrole nitrogen positions, with minor spin density at the β-pyrrole positions and even less spin density at the α-carbons.[29,46,47] Oxidation of a β-pyrrole-substituted porphyrin results in positive spin density at the α- and

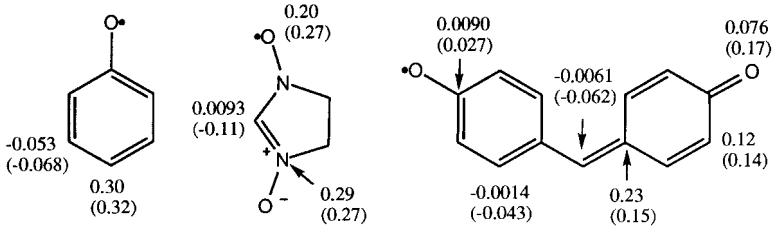


**Figure 4.** PM3-calculated and other calculated[47–50] spin densities for SCUs

 

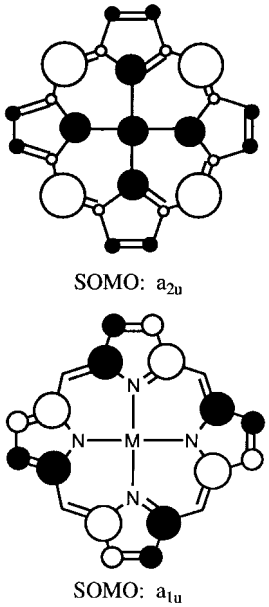


**Figure 5.** Porphyrin singly occupied molecular orbitals (SOMOs)

$\beta$-carbons and negative density at the *meso*-carbons.[52] Because of the large spin density at the *meso*-carbons of *meso*-substituted porphyrin radical cations, we employed our efforts to design porphyrin radical cation systems bearing SCUs attached at the *meso*-positions. Because of the steric demands at the *meso*-position of the porphyrin macrocycle, we investigated three different modifications of the porphyrin periphery: phenyl *meso*-substitution, ethenyl *meso*-substitution and ethynyl *meso*-substitution. Figure 6 shows the structures used in this study.

To begin the study, we determined the connectivity (or union mode) of the SCUs that leads to ferromagnetic coupling with the oxidized porphyrin. A useful approach to this determination is the starred–non-starred formalism. 'Starred' refers to positions of positive spin density and 'non-starred' refers to positions with no spin density (nodal positions) or negative spin density. It has been shown that union of an active site (starred position) with an inactive site (non-starred position) results in a high-spin ground state.[53]

First we will discuss the electronic properties of $ZnTPP^{+\cdot}$ and the oxy radical as the SCUs and the union modes leading to high-spin coupling. In $ZnTPP^{+\cdot}$, the spin at the *meso*-position can delocalize into *meso*-phenyl rings, as evidenced by proton hyperfine coupling in the EPR spectra of these systems.[46] The spin of the oxy radical delocalizes into the attached phenyl ring resulting in large positive spin density *para* to the oxygen (active site) and negative spin density *meta* to the oxygen (inactive sites).[25,26,48]

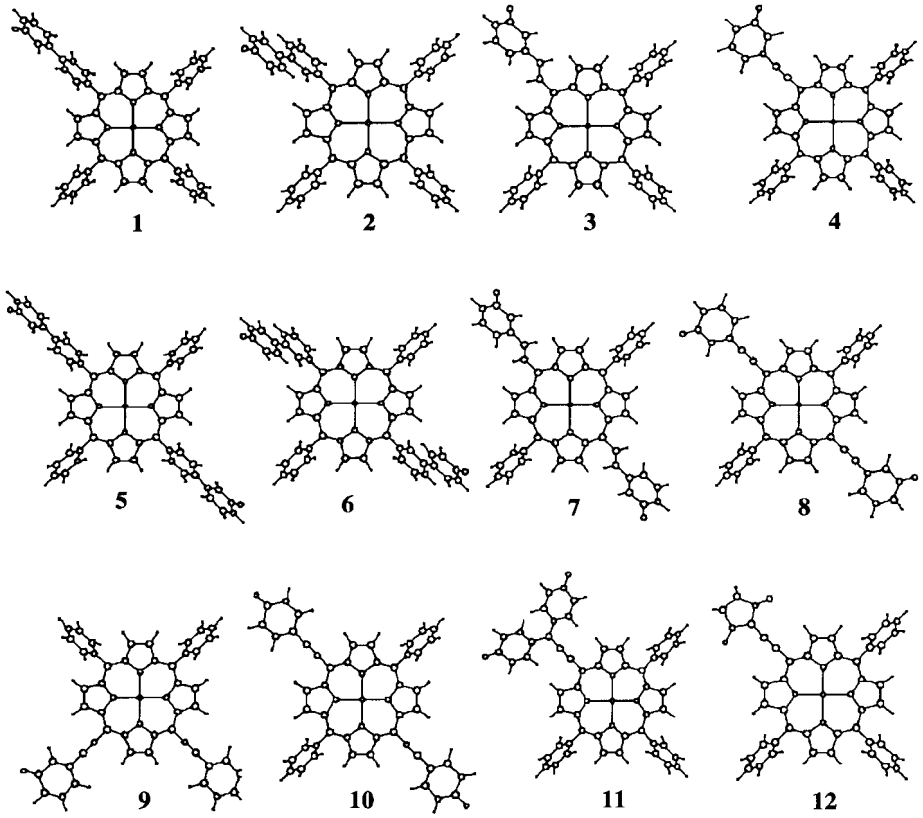


**Figure 6.** Porphyrin systems used in this study

 

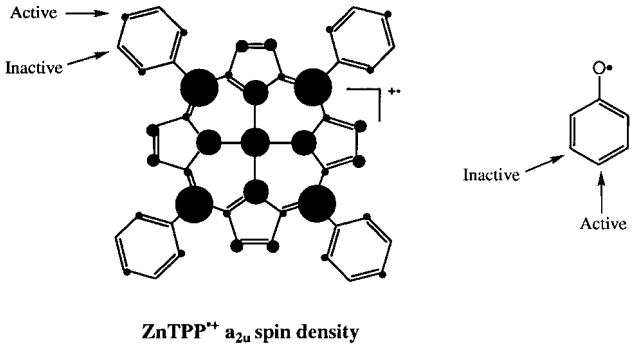


**Figure 7.** Active and inactive union sites for $ZnTPP^{+\cdot}$ and the SCU phenoxy radical

Given the existence of spin density in the phenyl rings of $ZnTPP^{+\cdot}$, we predict that the union of an inactive porphyrin phenyl position with an active SCU site or the union of an active porphyrin site with an inactive SCU site illustrated in Fig. 7 should both lead to ferromagnetic coupling. Compounds **1** and **5** have active-$TPP^{+\cdot}$–inactive-oxy union modes whereas **2** and **6** have inactive-$TPP^{+\cdot}$–active-oxy union modes.

After qualitatively determining which union modes lead to ferromagnetic coupling, we semiquantitatively investigated which connectivity provides the largest ferromagnetic coupling. It is convenient to use the '*meta*-through-a-benzene' union mode in examining the semiquantitative results for the $ZnTPP^{+\cdot}$–oxy study. The benzene ring which has the SCUs attached *meta* to each other is acting as the FCU (hereafter referred to as MBC: '*meta*-benzene coupler'). The magnitude of the coupling is reflected by the magnitude of the spin density in the MBC from each SCU.[54] A brief discussion of the coupling of *m*-xylylene will prove helpful. The biradical *m*-xylylene is composed of a benzene ring (the MBC) with two methylene radicals (the SCUs) attached *meta* to each other. As shown in Fig. 8 and Table 1, examination of various conformers of *m*-xylylene shows the relationship between MBC spin density and spin coupling.[55] When the two methylenes are planar (in the same plane as the MBC), both methylene radical spins can delocalize into the MBC and contribute equally to the spin density in the MBC, resulting in a large exchange interaction and a large singlet–triplet gap.

When one methylene is twisted perpendicular to the plane of the MBC while the other methylene remains planar, the spin density in the MBC comes mainly from delocalization of the planar methylene spin. The exchange interaction is dramatically decreased because the conformation keeps most of the two spins spatially separated. This illustrates that it is not sufficient to have atoms with large spin densities attached *meta*-through-a-benzene: the factor that determines the magnitude of the exchange interaction is the amount of spin density delocalized into the MBC from *each* SCU.[54,55] Separating the spin density in the MBC into its SCU components is a convenient means of rationalizing the spin coupling in our porphyrin radical cation–SCU systems. Therefore, two important identifications are needed to explain the calculated coupling trends in our $ZnTPP^{+\cdot}$–oxy systems: which benzene ring has the SCUs attached *meta* to each other (*i.e.* which ring is the MBC) and the amount of spin density in the MBC from each SCU.

In **1** the phenyl ring bearing the oxy radical is the MBC as shown in Fig. 9. However, for **2** the porphyrin phenyl ring is the MBC.

Next we consider the spin density from each SCU in the MBC. Since the connectivities of **1** and **2** do not allow the SCU spins to be resonance delocalized beyond the MBC, we can determine the amount of spin density in the MBC from each SCU. The results are displayed in Table 2.

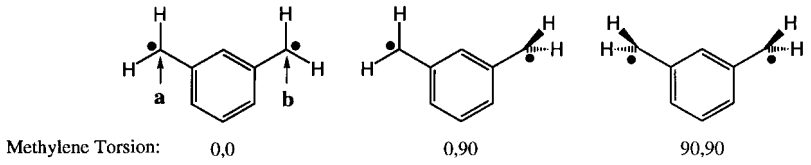


**Figure 8.** Labels and methylene torsion angles for *m*-xylylene

**Table 1.** UHF-PM3-calculated spin densities and singlet–triplet gaps for *m*-xylylene conformers

| Methylene torsion | $\Delta E_{LS-HS}$[a] (kcal $mol^{-1}$) | MBC spin density | MBC spin density from methylene **a** | MBC spin density from methylene **b** | Methylene **a** spin density | Methylene **b** spin density |
|---|---|---|---|---|---|---|
| 0,0 | 15.3 | 0.878 | 0.439 | 0.439 | 0.561 | 0.561 |
| 0,90 | 0.581 | 0.535 | 0.473 | 0.062 | 0.527 | 0.944 |
| 90,90 | −0.021 | 0.112 | 0.056 | 0.056 | 0.944 | 0.944 |

[a] Singlet–triplet energy gap. A positive value indicates a triplet ground state and a negative value a singlet ground state.

 

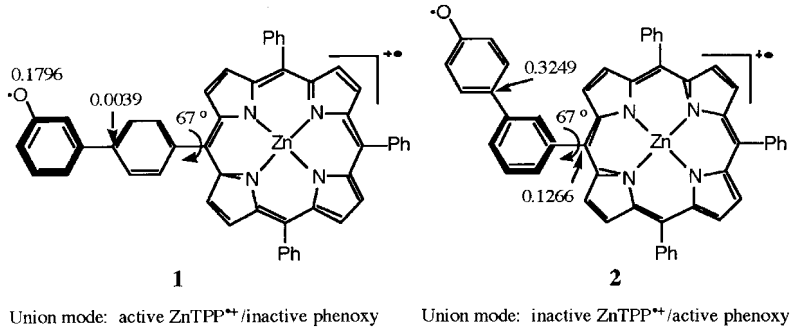


**Figure 9.** Active and inactive union sites for $TPP^{+\cdot}$ and the SCU phenoxy radical. The MBC is a different ring in each biradical and is shown in bold

The *para*-substituted $ZnTPP^{+\cdot}$ system **1** has a smaller exchange interaction than the *meta*-substituted $ZnTPP^{+\cdot}$ system **2**. Even though the *para*-substituted $ZnTPP^{+\cdot}$ system has a large amount of spin density in the MBC (0.8210), the spin mainly originates from *only one* of the SCUs—the oxy radical (0.8204). The tiny amount of spin density at the phenyl *para*-position is an indication that there is very little spin from the porphyrin radical cation in the coupler leading to a small exchange interaction in **1**. Conversely, the *meta*-substituted $ZnTPP^{+\cdot}$ system, **2**, has a smaller total spin density in the MBC (0.1516), but because it has contributions from both SCUs (0.017 from porphyrin radical cation and 0.13 from oxy radical) its exchange interaction is over twice as large. Thus, the results of the calculations indicate that the inactive porphyrin–active phenoxy union mode provides stronger coupling than the active porphyrin–inactive phenoxy union mode, illustrating an important design element.

The spin coupling in the phenyl *meso*-substituted porphyrin is limited by the phenyl-core torsion. Because the steric interactions between the $\beta$-pyrrole protons and the phenyl *ortho*-protons force the phenyl rings to twist considerably (between 60° and 70° for MTPP derivatives),[45,46] there is only a small amount of spin from the porphyrin radical cation delocalized into the porphyrin phenyl rings, thus limiting the spin–spin coupling.

Realizing the need for more delocalized spin from the macrocycle in the MBC to achieve larger exchange interactions, we investigated the ethenyl-bridged porphyrin **3** and the ethynyl-bridged porphyrin **4**. The $\beta$-ethenyl bridge proton also experiences steric interactions with the $\beta$-pyrrole proton, causing the bridge to twist by 50°, but the amount of spin delocalized from the porphyrin radical cation to the MBC is larger for ethene than for phenyl, as shown in Table 2.

Calculations show that because the ethynyl linkage allows elimination of the torsion factor allowing the planar alignment of phenoxy ring with the porphyrin radical cation, the singlet–triplet gap in **4** is nearly 380 cal $mol^{-1}$ greater than that in **3**. Hence the magnitude of the exchange interaction is shown to be a function of the amount of spin density from $ZnTPP^{+\cdot}$, the smallest contributor to the MBC spin density.

Next, we investigated redox-activated exchange coupling—the effectiveness of the $ZnTPP^{+\cdot}$ to exchange couple two SCUs. Other research groups have investigated redox-activated high-spin species.[56–60] Examination of the quartet–doublet gaps for **5–8** in Table 2 shows that high-spin ground states are achieved consistent with the trends for biradicals **1–4**, *i.e.* the exchange coupling increases in the order $\mathbf{5} < \mathbf{6} < \mathbf{7} < \mathbf{8}$. Since the quartet state is calculated to be the ground state for these

**Table 2.** $ZnTPP^{+\cdot}$–oxy spin–spin coupling and spin density analysis[a]

| Porphyrin | $\Delta E_{LS-HS}$[b] (kcal $mol^{-1}$) | MBC spin density | MBC spin density from $ZnTPP^{+\cdot}$ | MBC spin density from oxy radical |
|---|---|---|---|---|
| **1** | 0.067 (TGS) | 0.8210 | 0.0006 | 0.8204 |
| **2** | 0.149 (TGS) | 0.1516 | 0.0171 | 0.1345 |
| **3** | 0.903 (TGS) | 0.8362 | 0.0187 | 0.8175 |
| **4** | 1.282 (TGS) | 0.8425 | 0.0237 | 0.8188 |
| **5** | 0.041 (QGS) | 0.8211 | 0.0001 | 0.8210 |
| **6** | 0.070 (QGS) | 0.1529 | 0.0167 | 0.1362 |
| **7** | 0.309 (QGS) | 0.8276 | 0.0094 | 0.8182 |
| **8** | 0.405 (QGS) | 0.8323 | 0.0131 | 0.8192 |
| **9** | 0.405 (QGS) | 0.8324 | 0.0133 | 0.8192 |

[a] TGS = triplet ground state for $S = 1$ biradical; QGS = quartet ground state for $S = 3/2$ triradical.
[b] $\Delta E_{LS-HS}$ = high-spin–low-spin energy gap; positive value indicates a high-spin ground state.

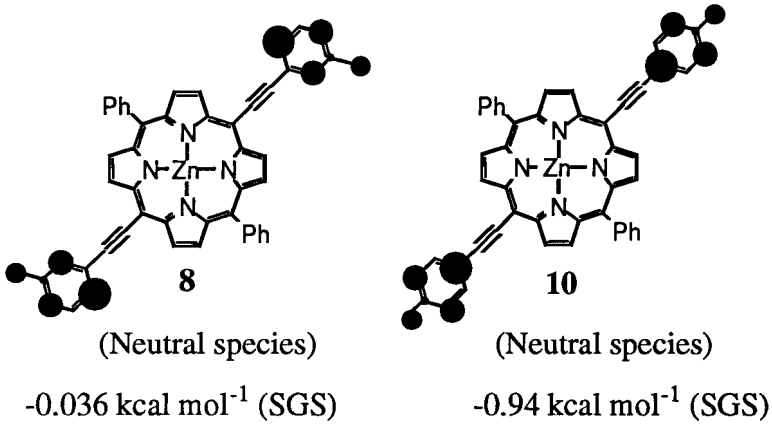


**Figure 10.** Spin densities and high-spin–low-spin energy gaps for biradicals **8** and **10**

**Table 3.** Neutral porphyrin–Oxy high-spin–low-spin energy gaps[a]

| Porphyrin | $\Delta E_{LS-HS}$[a] (kcal mol$^{-1}$) |
|---|---|
| **5** | 0 |
| **6** | 0 |
| **7** | −0.017 |
| **8** | −0.036 |
| **9** | −0.024 |
| **10** | −0.936 |

triradicals, the calculations predict the porphyrin radical cation functions as a high-spin coupler. We believe similar trends would be observed for species having three or four SCUs attached to $ZnTPP^{+\cdot}$.

We also performed calculations on the neutral, unoxidized porphyrin core to test its effectiveness as a ferromagnetic coupler, and the results are presented in Table 3. The lack of interaction between the peripheral SCUs of **5** and **6**, evidenced by the degenerate ground states, and the small antiferromagnetic coupling of the ethenyl- and ethynyl-bridged systems, **7** and **8**, demonstrates, as expected, the ineffectiveness of the neutral porphyrin as an FCU. Since both SCUs are attached at nodal positions, very little spin is delocalized into the macrocycle. Spin polarization in **7** and **8** may be responsible for the low-spin ground-state preference. Therefore, porphyrin radical cation enhances exchange coupling among SCUs, and could prove to be an important redox-activated exchange coupling fragment.

The neutral porphyrin is more effective as an antiferromagnetic coupler as seen in system **10**. In contrast to the connectivity of **8** (neutral species), the active phenoxy position of **10** is attached to the porphyrin phenyl ring as shown in Fig. 10. The ZnTPP antiferromagnetically couples the two spins leading to a singlet ground state.

After determining the most effective means of accomplishing ferromagnetic coupling, we turned our attention to the peripheral SCUs. Galvinoxyl and nitronylnitroxide are both stable radical moieties which have been incorporated in other systems exhibiting magnetic interactions.[61–65] Using the ethynyl-bridged derivative, we compared these two SCUs to see which would give the largest exchange interaction.

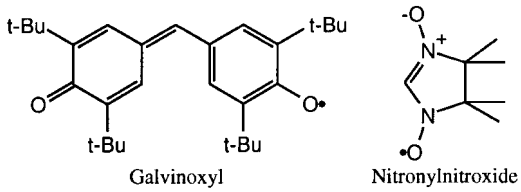


The FCU in these systems is not the MBC since there is no benzene ring with SCUs attached *meta* to each other. There is, however, another robust ferromagnetic coupler intrinsic in these systems—trimethylenemethane (TMM). Just as we used the *meta*-through-a-benzene motif to examine the coupling strength for the oxy-substituted radical cation porphyrin systems, we now use the TMM motif to examine the coupling strength in the galvinoxyl- and nitronylnitroxide-substituted radical cation porphyrin systems. We examined the spin components of the TMM coupler to rationalize the trend of the exchange interaction just as we did with the *meta* benzene coupler.

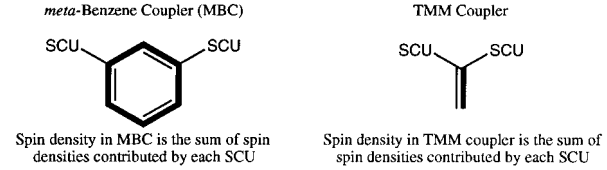


As shown in Fig. 11, the galvinoxyl-substituted porphyrin has more spin density from the porphyrin radical cation contributing to the TMM coupler (the bold double bond) than the nitronylnitroxide derivative,

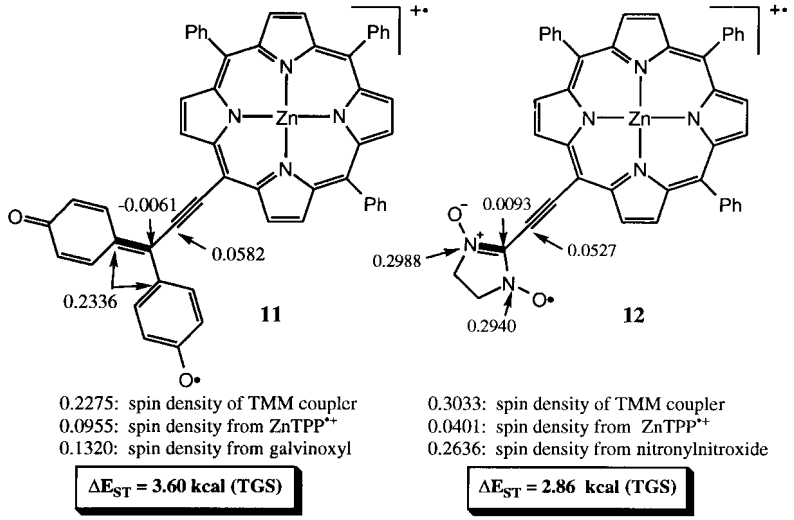


**Figure 11.** Spin densities and high-spin–low-spin energy gaps for galvinoxyl- and nitronylnitroxide-substituted porphyrins

whereas the nitronylnitroxide derivative has more spin density from the SCU contributing to the TMM coupler. Consistent with the results of the *meta* benzene coupler, the exchange interaction is limited by delocalized spin density from the smaller contributor.

In conclusion, these calculations support the feasibility of using the porphyrin radical cation as an efficient FCU to build high-spin species. The trends in computed high-spin–low-spin energy gaps were explained with the aid of a coupler–spin analysis. Even though the *meta*-substituted $ZnTPP^{+\cdot}$ system is calculated to have a larger exchange interaction than the *para*-substituted $ZnTPP^{+\cdot}$ system, the exchange interaction is limited by the phenyl torsion which modulates delocalization of the spin from the $ZnTPP^{+\cdot}$ into the MBC. The ethenyl- and ethynyl-bridged systems, however, have two factors contributing to their larger exchange interactions compared with the phenyl-bridged systems: decreased torsion (50° twist for ethenyl and 0° twist for ethynyl) and a smaller number of atoms in the bridge over which the spin is delocalized. The ethynyl-bridged system has the largest spin contributions from both SCUs in the MBC and hence the largest exchange interaction. The importance of the redox-activated spin coupling was demonstrated by the lack of significant ferromagnetic coupling when the unoxidized ZnTPP was used as the FCU (*i.e.* $ZnTPP^{+\cdot}$ *vs* ZnTPP). Finally, galvinoxylethynyl substitution results in greater coupling than nitronylnitroxide–ethynyl coupling.

## Acknowledgments

This work was funded by the National Science Foundation (CHE-9501085) under the CAREER Program and by Research Corporation (CS0127) under the Cottrell Scholars Program. K.A.S. thanks the Department of Education for an Electronic Materials Fellowship.

## REFERENCES

1. (a) E. Coronado, P. Delhaes, D. Gatteschi and J. S. Miller. *Molecular Magnetism: from Molecular Assemblies to the Devices*. Kluwer, Dordrecht (1996); and (b) D. Gatteschi. *Molecular Magnetic Materials*. Kluwer, Dordrecht (1991); and (c) O. Kahn. *Molecular Magnetism*. VCH, New York (1993); and (d) A. Rajca. *Chem. Rev.* **94,** 871 (1994); (e) M. M. Turnbull, T. Sugimoto and L. K. Thompson. *Molecule-Based Magnetic Materials, Theory, Techniques, and Applications*, ACS Symposium Series, No. 644. American Chemical Society, Washington, DC (1996); and (f) C. J. O'Connor. *Research Frontiers in Magnetochemistry*. World Scientific, Singapore (1993).
2. J. S. Miller and A. J. Epstein. *Angew. Chem. Int. Ed. Engl.* **33,** 385 (1994).
3. H. Iwamura. *Pure Appl. Chem.* **65,** 57 (1993).
4. T. Akita, Y. Mazaki and K. Kobayashi. *J. Chem. Soc., Chem. Commun.* 1861 (1995).
5. T. Akita and K. Kobayashi. *Adv. Mater.* **9,** 346 (1997).
6. M. M. Matsushita, A. Izuoka, T. Sugawara, T. Kobayashi, N. Wada, N. Takeda and M. Ishikawa. *J. Am. Chem. Soc.* **119,** 4369 (1997).
7. D. Gatteschi. *Adv. Mater.* **6,** 635 (1994).
8. J. S. Miller and A. J. Epstein. *Angew. Chem. Int. Ed. Engl.* **33,** 385 (1994).
9. T. Kaneko, S. Toriu, E. Tsuchida, H. Nishide, D. Yamaki, G. Maruta and K. Yamaguchi. *Chem. Lett.* 421 (1995).
10. S. Rajca and A. Rajca. *J. Am. Chem. Soc.* **117,** 9172 (1995).
11. H. Nishide, T. Kaneko, T. Nii, K. Katoh, E. Tshuchida and P. Lahti. *J. Am. Chem. Soc.* **118,** 9695 (1996).
12. D. A. Dougherty. *Acc. Chem. Res.* **24,** 88 (1991).
13. H. Iwamura. *Adv. Phys. Org. Chem.* **26,** 179 (1990).
14. N. Koga and H. Iwamura. *Nihon Kagaku Naishi*, 1456 (1989).
15. M. Kamachi. *Nihon Butsuri Gakkaishi* **42,** 351 (1987).
16. M. Kitano, N. Koga and H. Iwamura. *J. Chem. Soc., Chem. Commun.* 447 (1994).
17. J. S. Miller, J. C. Calabrese, R. S. McLean and A. J. Epstein. *Adv. Mater.* **4,** 498 (1992).
18. (a) D. A. Summerville, T. W. Cape, E. D. Johnson and F. Basolo. *Inorg. Chem.* **17,** 3297 (1978); (b) K. Nagai, T. Iyoda, A. Fujishima and K. Hashimoto. *Syn. Metals*, **85,** 1701 (1997); for papers discussing novel porphyrins, high-spin porphyrins and porphyrinic magnetic materials, see Refs 19 and 20 and the following: (c) B. J.

 

Conklin, S. P. Sellers, J. P. Fitzgerald and G. T. Yee. *Adv. Mater.* **6,** 836 (1994); and (d) H. Iwamura. *Adv. Phys. Org. Chem.* **26,** 179 (1990); and (e) M. Kamachi. *Nihon Butsuri Gakkaishi* **42,** 351 (1987); (f) M. Kitano, N. Koga and H. Iwamura. *J. Chem. Soc., Chem. Commun.* 447 (1994); (g) M. Kitano, Y. Ishimaru, K. Inoue, N. Koga and H. Iwamura. *Inorg. Chem.* **33,** 6012 (1994); (h) N. Koga and H. Iwamura. *Nihon Kagaku Naishi* 1456 (1989).
19. D. A. Shultz, D. A. Knox, L. W. Morgan, K. Sandberg and G. N. Tew. *Tetrahedron Lett.* **34,** 3975 (1993).
20. D. A. Shultz, K. P. Gwaltney and H. Lee. *J. Org. Chem.* **63,** 769 (1998); D. A. Shultz, K. P. Gwaltney and H. Lee. *J. Org. Chem.*, **63,** 7584 (1998).
21. A. S. Ichimura, N. Koga and H. Iwamura. *J. Phys. Org. Chem.* **7,** 207 (1994).
22. P. M. Lahti, A. R. Rossi and J. A. Berson. *J. Am. Chem. Soc.* **107,** 2273 (1985).
23. P. M. Lahti and A. S. Ichimura. *Mol. Cryst. Liq. Cryst.* **176,** 125 (1989).
24. P. M. Lahti. *Int. J. Quant. Chem.* **44,** 785 (1992).
25. P. M. Lahti and A. S. Ichimura. *J. Org. Chem.* **56,** 3030 (1991).
26. P. M. Lahti, A. S. Ichimura and J. A. Berson. *J. Org. Chem.* **54,** 958 (1989).
27. N. Yoshioka, P. M. Lahti, T. Kaneko, Y. Kuzumaki, E. Tsuchida and H. Nishide. *J. Org. Chem.* **59,** 4272 (1994).
28. C. H. Reynolds. *J. Org. Chem.* **53,** 6061 (1988).
29. K. Prendergast and T. G. Spiro. *J. Phys. Chem.* **95,** 9728 (1991).
30. A. G. Skillman, J. R. Collins and G. H. Loew. *J. Am. Chem. Soc.* **114,** 9538 (1992).
31. O. Brigaud, P. Battioni and D. Mansuy. *New J. Chem.* **16,** 1031 (1992).
32. T. Takeuchi, H. B. Gray and W. A. Goddard III. *J. Am. Chem. Soc.* **116,** 9730 (1994).
33. M. Minato, P. M. Lahti and H. van Willigen. *J. Am. Chem. Soc.* **115,** 4532 (1993).
34. *AMPAC Version 5.0.* Semichem, Summit, Shawnee, KS (1994).
35. P. G. Gassman, A. Ghosh and J. Almlof. *J. Am. Chem. Soc.* **114,** 9990 (1992).
36. S. M. LeCours, S. G. DeMagno and M. J. Therien. *J. Am. Chem. Soc.* **118,** 11854 (1996).
37. S. Rao and V. Krishnan. *J. Mol. Struct.* **327,** 279 (1994).
38. W. R. Scheidt, M. E. Kastner and K. Hatano. *Inorg. Chem.* **17,** 706 (1978).
39. Ruffled and saddled conformations for $MTPP^{+\cdot}$ often are observed experimentally; see, for example, H. Song, C. A. Reed and W. R. Scheidt. *J. Am. Chem. Soc.* **111,** 6865 (1989).
40. W. T. Bordern, E. R. Davidson and D. F. Feller. *Tetrahedron*, **38,** 737 (1982).]
41. R. Timkovich and A. Tulinsky. *J. Am. Chem. Soc.* **91,** 4430 (1969).
42. We replaced Mg with Zn because we are synthesizing a variety of radical-substituted Zn(II) porphyrins; See refs 19 and 20.
43. E. B. Fleischer. *Acc. Chem. Res.* **3,** 105 (1970).
44. M. D. Glick, G. H. Cohen and J. L. Hoard. *J. Am. Chem. Soc.* **89,** 1996 (1967).
45. L. D. Spaulding, P. G. Eller, J. A. Bertrand and R. H. Felton. *J. Am. Chem. Soc.* **96,** 982 (1974).
46. J. Fajer, D. C. Borg, A. Forman, D. Dolphin and R. H. Felton. *J. Am. Chem. Soc.* **92,** 3451 (1970).
47. M. Atamian, R. W. Wagner, J. L. Lindsey and D. F. Bocian. *J. Am. Chem. Soc.* **27,** 1510 (1988).
48. B. S. Prabhananda. *J. Chem. Phys.* **79,** 5752 (1983).
49. A. Zheludev, V. Barone, M. Bonnet, B. Delley, A. Grand, E. Ressouche, P. Rey, R. Subra and J. Schweizer. *J. Am. Chem. Soc.* **116,** 2019 (1994).
50. K. Mukai, T. Kamata, T. Tamaki and K. Ishizu. *Bull. Chem. Soc. Jpn.* **49,** 3376 (1976).
51. G. R. Luckhurst. *Mol. Phys.* **11,** 205 (1966).
52. H. Fujii. *J. Am. Chem. Soc.* **115,** 4641 (1993).
53. D. E. Seeger, P. M. Lahti, A. R. Rossi and J. A. Berson. *J. Am. Chem. Soc.* **108,** 1251 (1986).
54. J. Zhang and M. Baumgarten. *Chem. Phys.* **214,** 291 (1997).
55. S. Fang, M. -S. Lee, D. A. Hrovat and W. T. Borden. *J. Am. Chem Soc.* **117,** 6727 (1995).
56. H. Sakurai, R. Kumai, A. Izuoka and T. Sugawara. *Chem. Lett.* 879 (1996).
57. M. M. Wienk and R. A. J. Janssen. *J. A. Chem. Soc.* **118,** 10626 (1996).
58. M. M. Wienk and R. A. J. Janssen. *J. Am. Chem. Soc.* **119,** 4492 (1997).
59. K. R. Stickley and S. C. Blackstock. *J. Am. Chem. Soc.* **116,** 11576 (1994).
60. K. R. Stickley, T. D. Selby and S. C. Blackstock. *J. Org. Chem.* **62,** 448 (1997).
61. H. Nishide, N. Yoshioka, T. Kaneko and E. Tsuchida. *Macromolecules* **23,** 4487 (1990).
62. Y. Miura, K. Inui, F. Yamaguchi, M. Inoue, Y. Teki, T. Takui and K. Itoh. *J. Polym. Sci. A* **30,** 959 (1992).
63. K. Awaga and Y. Maruyama. *J. Chem. Phys.* **91,** 2743 (1989).
64. A. Caneschi, D. Gatteschi, P. Rey and R. Sessoli. *Inorg. Chem.* **27,** 1756 (1988).
65. A. Caneschi, D. Gatteschi, J. P. Renard, P. Rey and R. Sessoli. *Inorg. Chem.* **28,** 1976 (1989).

 